ARTICLE
Journal of Cellular Biochemistry 112:2850–2864 (2011)

Journal of Cellular Biochemistry

Cisplatin Treatment of Primary and Metastatic Epithelial Ovarian Carcinomas Generates Residual Cells With Mesenchymal Stem Cell–Like Profile

Ardian Latifi,[1,2] Khalid Abubaker,[1,2] Natalie Castrechini,[1] Alister C. Ward,[3] Clifford Liongue,[3] Francoise Dobill,[1] Janani Kumar,[3] Erik W. Thompson,[2,4] Michael A. Quinn,[1,5] Jock K. Findlay,[1,5,6] and Nuzhat Ahmed[1,2,5,6]*

[1]*Women's Cancer Research Centre, Royal Women's Hospital, Victoria 3052, Australia*
[2]*University of Melbourne Department of Surgery, St Vincent Hospital, Victoria 3065, Australia*
[3]*School of Medicine, Deakin University, Victoria 3217, Australia*
[4]*St. Vincent's Institute, Victoria 3065, Australia*
[5]*Department of Obstetrics and Gynaecology, University of Melbourne, Victoria 3052, Australia*
[6]*Prince Henry's Institute of Medical Research, Victoria 3168, Australia*

ABSTRACT

Epithelial mesenchymal transition (EMT) and cancer stem cells (CSC) have been associated with resistance to chemotherapy. Eighty percent of ovarian cancer patients initially respond to platinum-based combination therapy but most return with recurrence and ultimate demise. To better understand such chemoresistance we have assessed the potential role of EMT in tumor cells collected from advanced-stage ovarian cancer patients and the ovarian cancer cell line OVCA 433 in response to cisplatin in vitro. We demonstrate that cisplatin-induced transition from epithelial to mesenchymal morphology in residual cancer cells correlated with reduced E-cadherin, and increased N-cadherin and vimentin expression. The mRNA expression of Snail, Slug, Twist, and MMP-2 were significantly enhanced in response to cisplatin and correlated with increased migration. This coincided with increased cell surface expression of CSC-like markers such as CD44, α2 integrin subunit, CD117, CD133, EpCAM, and the expression of stem cell factors Nanog and Oct-4. EMT and CSC-like changes in response to cisplatin correlated with enhanced activation of extracellular signal-regulated kinase (ERK)1/2. The selective MEK inhibitor U0126 inhibited ERK2 activation and partially suppressed cisplatin-induced EMT and CSC markers. In vivo xenotransplantation of cisplatin-treated OVCA 433 cells in zebrafish embryos demonstrated significantly enhanced migration of cells compared to control untreated cells. U0126 inhibited cisplatin-induced migration of cells in vivo, suggesting that ERK2 signaling is critical to cisplatin-induced EMT and CSC phenotypes, and that targeting ERK2 in the presence of cisplatin may reduce the burden of residual tumor, the ultimate cause of recurrence in ovarian cancer patients. J. Cell. Biochem. 112: 2850–2864, 2011.

KEY WORDS: OVARIAN CARCINOMA; CISPLATIN RESISTANCE; CANCER STEM CELL; EPITHELIAL MESENCHYMAL TRANSITION; METASTASIS

Epithelial ovarian cancer (EOC) kills approximately 115,000 women annually worldwide. Surgery followed by chemotherapy is the primary initial treatment in most advanced-stage patients. Current treatment with cisplatin {*cis*-diamminedichloroplatinum(II)} or platinum-based analogs like carboplatin in combination with paclitaxel results in a complete remission in 80% of patients [Ozols, 2006]. Unfortunately, remission is usually short lived with subsequent recurrence due to chemoresistance, and death as a consequence of metastatic spread. The phenomenon of acquired chemotherapy resistance in ovarian carcinomas has been

Ardian Latifi and Khalid Abubaker contributed equally to this work.

Additional supporting information may be found in the online version of this article.

Grant sponsor: Royal Women's Hospital Foundation; Grant sponsor: Women's Cancer Foundation; Grant sponsor: National Health and Medical Research Council of Australia; Grant number: RegKey#441101; Grant sponsor: Victorian Breast Cancer Research Consortium.

*Correspondence to: Dr. Nuzhat Ahmed, Women's Cancer Research Centre, Royal Women's Hospital, 20 Flemington Road, Parkville, VIC 3052, Australia. E-mail: nuzhat.ahmed@thewomens.org.au

Received 13 May 2011; Accepted 16 May 2011 • DOI 10.1002/jcb.23199 • © 2011 Wiley-Liss, Inc.
Published online 26 May 2011 in Wiley Online Library (wileyonlinelibrary.com).

recognized for decades but the problem remains unsolved. Hence, a more detailed understanding of the molecular mechanisms by which tumor cells survive chemotherapy treatment is likely to lead to novel therapeutic targets with successful outcomes.

Emerging lines of evidence have associated chemoresistance with acquisition of epithelial mesenchymal transition (EMT) in cancer [Wang et al., 2009]. These processes are also believed to correlate with a ''cancer stem cell (CSC)-like'' phenotype as demonstrated recently in vivo by the mesenchymal and ''tumor initiating'' phenotypes of the residual tumor cells in breast cancer patients that survived conventional therapy [Kim et al., 2009]. EMT is a developmental process and is hypothesized to play an important role in tumor progression and metastasis in diverse cancers, including ovarian cancer [Ahmed et al., 2007; Guarino et al., 2007]. The hallmark of EMT is the loss of E-cadherin which is mediated by mutation or promoter methylation of CDH1, or direct promoter repression mediated by the transcription factors Snail, Slug (Snail 2), Twist, Zeb-1, and Sip 1 (Zeb-2) [Lombaerts et al., 2006; Peinado et al., 2007]. In parallel, there is a replacement by mesenchymal-type adhesion molecules (for example N-cadherin) and cytoskeletal filaments (for example vimentin). Several clinical studies have shown a correlation between decreased expression of E-cadherin and poor survival in patients with different tumor types [Uchikado et al., 2005]. Consistent with that, there is evidence that silencing of E-cadherin repressors by small interfering RNAs may increase the sensitivity of tumor cells to chemotherapy [Kajita et al., 2004], suggesting a strong link between EMT and chemoresistance.

Cytotoxicity produced by cisplatin has been shown to be a consequence of DNA damage caused by the formation of cisplatin–DNA adducts [Sedletska et al., 2005]. In parallel, there are several DNA repair systems involved in the repair of cisplatin–DNA adducts [Jayachandran et al., 2010] and activation of p53 and several other pathways have been shown to be involved [Perego et al., 1996; Ohmichi et al., 2005], but the underlying mechanism(s) which specifically dictate tumor cell survival after treatment with cisplatin still remain unknown. Cisplatin-induced genotoxic stress induces activation of multiple signal transduction pathways [Mabuchi et al., 2004; Leong et al., 2007], among which are members of mitogen activated protein kinase (MAPK) pathways [Brozovic and Osmak, 2007]. Activation of JNK and ERK1/2 has been demonstrated in ovarian cancer cell lines in response to cisplatin [Cui et al., 2000]. A recent study has demonstrated high basal levels of nuclear ERK2 in cisplatin-resistant ovarian cancer cell lines [Lee et al., 2007]. Inhibition of ERK1/2 has also been shown to sensitize ovarian cancer cells to cisplatin [Hayakawa et al., 2000], suggesting a role of ERK1/2 as a mediator of pro-survival signals in cisplatin-resistant population.

In this study, we investigated the potential role of EMT in cisplatin-induced resistance in ovarian carcinomas. Cisplatin enhanced activation of ERK2 and induced EMT and CSC-like phenotypes in ovarian cancer cells. Inhibition of ERK2 activation by a specific MEK inhibitor resulted in the partial suppression of EMT and stemness proteins. These results were confirmed in vivo using a zebrafish xenotransplantation model in which cisplatin-induced enhanced migration was abrogated with a selective MEK inhibitor. Our results identify a novel mechanism by which ERK-EMT-CSC signaling protects ovarian carcinoma cells against the cytotoxic effects of cisplatin and suggest that targeting ERK-EMT-CSC pathways in combination with chemotherapy may decrease the propensity of residual tumor which are the ultimate cause of recurrence.

MATERIALS AND METHODS

CLINICAL DESCRIPTION OF PATIENTS RECRUITED IN THE STUDY

Primary ovarian tumors (PT) were obtained from advanced-stage patients diagnosed with serous, endometriod, and clear cell carcinomas (Table I). Ascites (As) were collected from patients diagnosed with advanced-stage serous ovarian carcinoma. The clinical description of the patients is described in Table I. The histopathological diagnosis, tumor grades, and stages were determined by staff pathologists as part of the clinical diagnosis and were determined by the method described previously [Silverberg, 2000]. Malignant ascites were obtained during the surgery in patients with primary carcinoma, as well as at the time of recurrence. The study was approved by the Research and Human Ethics Committee (HEC # 09/09) of The Royal Women's Hospital, Melbourne, Australia.

TABLE I. Clinical Description of Patients Involved in the Study

Patient number	Tissue type	Tumour subtype	Stage	Age	Treatment	Experimental methods used
1	PT	Serous	IIIc	64	None	WB, FC, IF
3	PT	Clear cell Carcinoma	III	60	None	WB, q-PCR
4	PT	Endometroid	IIIc	51	None	WB, q-PCR
7	PT	Serous	IIc	57	None	q-PCR
8	PT	Serous	III	72	None	q-PCR
9	PT	Serous	III	59	None	IF, WB, q-PCR
18	PT	Serous	III	62	None	IF
2A	As	Serous	IIIc	51	Docetaxel 3 cycles, carboplatin and paclitaxel 6 cycles, doxorubicin 3 cycles, gemcitabine and carboplatin 6 cyles, docetaxel 3 cycles, and topotecan 2 cycles	FC, q-PCR, IF
3	As	Serous	IIIb	65	Carboplatin and paclitaxel 6 cycles	FC, q-PCR, IF, WB
5	As	Serous	IIIc	79	Cyclophosphamide 4 cycles, carboplatin 2 cycles, and docetaxel 1 cycle	FC, q-PCR, IF, WB
13	As	Serous	IIIc	59	None	FC, q-PCR, IF
19	As	Serous	IIIc	74	None	FC, IF, q-PCR
31	As	Serous	IIIc	NA	None	WB

PREPARATION OF TUMOR CELLS FROM ADVANCED-STAGE CARCINOMAS

Tumor sections of 0.2–0.4 g were cut into small pieces and incubated in growth medium consisting of DMEM and F12 Nutrient Ham (1:1) (Invitrogen, Melbourne, Australia) supplemented with heat inactivated fetal bovine serum [FBS, 10% (v/v)], glutamine (2 mM), hyaluronidase, and collagenase (300 U/ml) (Sigma, Sydney, Australia) at 37°C in 5% CO_2. After 1–2 weeks, confluent cultures were screened for fibroblast surface protein (FSP), CA-125, and epithelial cell adhesion molecule (EpCAM). Sustained expression of CA-125 and EpCAM was observed in 3–4 passage cultures with significantly low expression of FSP indicating the overriding dominance of epithelial tumor cells with very few contaminating cells expressing FSP. Primary overian tumor cells (PTs) were used between 3 and 4 passages.

PREPARATION OF TUMOR CELLS FROM ASCITES OF OVARIAN CANCER PATIENTS

Tumor cells were prepared as described previously [Ahmed et al., 2010b]. Briefly, cells were collected from 100 to 500 ml of ascites, and contaminating red blood cells were removed by hypotonic shock in sterile MilliQ H_2O. After 1–2 weeks in growth medium relatively pure tumor cells (ATs) were obtained [Ahmed et al., 2010b]. ATs were used between passages 3 and 6.

CELL LINES

The human epithelial ovarian cancer line OVCA 433 was generously provided by Dr. Robert Bast Jr. (MD Anderson Cancer Centre, Houston, TX) and was grown as described previously [Ahmed et al., 2002]. This cell line has been described previously [Ning et al., 2005].

ANTIBODIES AND REAGENTS

Monoclonal and polyclonal antibodies against CA125, FSP, CD44, CD24, CD117, CD133, and α2 integrin subunit were obtained from Millipore (Melbourne, Australia). Monoclonal antibody against N-cadherin was obtained from Zymed Laboratories (San Francisco). Polyclonal antibodies against E-cadherin, vimentin, Oct-4, Nanog, EpCAM, phospho-Erk1/2, and total-(T)-Erk2 were obtained from Cell Signalling Technology (Beverly, MA). U0126 was obtained from Merck (Melbourne, Australia).

CISPLATIN TREATMENT OF OVARIAN CANCER CELLS

Ovarian cancer cell line OVCA 433, PTs, and ATs were treated with cisplatin concentrations at which 50% growth inhibition was obtained (GI50), for 3–5 days. Ovarian cancer cell line OVCA 433 was treated with cisplatin (5–10 μg/ml) for 5 days while the primary tumors were treated with 1 μg/ml of cisplatin for 3 days. Chemonaive ascites tumor cells were treated with 2.5 μg/ml and chemoresistant ascites tumor cells with 5–10 μg/ml of cisplatin for 5 days. In another approach, OVCA 433 cell line was treated with 5 μg/ml of cisplatin for 4 days and then incubated in normal medium for 3 days. The cells were treated with the same concentration of cisplatin for another 3 days before experiments. These cells were termed ST (short-term treatment). OVCA 433 was also treated with cisplatin (5 μg/ml) for a month. Residual cells were maintained in the growth medium for 12–15 passages. These cells were termed LT (long-term treatment) [Ahmed et al., 2010a]. These approaches were taken to check the validity of cisplatin-treated phenotype and also to mimic the in vivo situation after multiple cycles of chemotherapy.

PROLIFERATION ASSAY

^{3}[H]-Thymidine uptake assay was performed as described previously [Kunimura et al., 1998]. The samples were analyzed using a β-counter (Hidex 300SL, LKB Instruments, Australia).

SDS–PAGE AND WESTERN BLOT (WB) ANALYSIS

SDS–PAGE and WB were performed as described previously [Ahmed et al., 2003]. Protein loading was monitored by stripping the membrane with Re-Blot solution (Chemicon International, Temecula, CA) and re-probing the membrane with β-actin primary antibody (Sigma–Aldrich, Sydney, Australia).

PREPARATION OF TUMOR CONDITIONED MEDIUM

Cells were seeded at 1×10^6 cells/25 cm^2 flask and allowed to grow in the growth medium for 24 h. A flask was treated with cisplatin (5 μg/ml) and the other was kept as control untreated cells. After 4 days, flasks were washed with medium lacking FBS and maintained in FBS free medium for 24 h after which the conditioned medium was collected and cleared of cells by centrifugation (2,000*g* for 10 min). Conditioned medium was concentrated 20-fold using Biomax Ultrafree Centrifugal Filter Unit (Millipore) with a 10-kDa pore diameter cut-off. To ensure equal loading, protein estimation was performed by Bradford protein assay kit (Pierce, Rockford).

ZYMOGRAPHY

Pro-MMP-2 and Pro-MMP-9 expression in conditioned medium were analyzed using 10% SDS–gelatin (2 mg/ml final concentration) zymography under nonreducing conditions. Conditioned medium were mixed with zymogram sample buffer (Biorad, PA) at 1:4 ratio. Following electrophoresis, gels were washed in 2.5% Triton X-100 (Sigma, NSW, Australia) then with distilled water to remove SDS. Gels were incubated at 37°C for 48 h in the incubation buffer (50 mM Tris–HCl, 5 mM $CaCl_2$, pH 7), stained with 0.05% Coomassie Blue R250 (Biorad) at room temperature and destained with the same solution without the Coomassie Blue. Gelatin degraded enzymes were identified as clear bands against a blue background. Human first-trimester cytotrophoblast cell line, HTR8/SVneo-cell conditioned medium (RPMI1640, FCS10%, PenStrep 100 U, L-Glutamine 2 mM) was used as a positive control [Lala et al., 2002].

IMMUNOFLUORESCENCE (IF) ANALYSIS

IF analysis of EMT and CSC markers was performed as described previously [Colomiere et al., 2009]. Images were captured by the photo multiplier tube using the Leica TCS SP2 laser, and viewed on a HP workstation and the Leica microsystems TCS SP2 software.

FLOW CYTOMETRIC (FC) ANALYSIS

FC method was used as described previously [Ahmed et al., 2002]. Briefly, untreated or cisplatin-treated cells were collected and rinsed

twice with PBS. Cells (10^6) were incubated with primary antibody for 1 h at 4°C and excess unbound antibody was removed by washing twice with PBS. Cells were stained with secondary antibody conjugated with phycoerythrin for 20 min at 4°C, washed twice with PBS and then re-suspended in 0.5 ml phosphate buffered saline (PBS) prior to FC analysis. In each assay background staining was detected using an antibody-specific IgG isotype. All data were analyzed using Cell Quest software (Becton-Dickinson, Bedford, MA). Results are expressed as mean intensity of fluorescence (MIF).

CELL MIGRATION ASSAY

The migratory potential of cells was assessed by the wound-healing assay as described previously [Ahmed et al., 2010a]. Photos were taken of the scratches at 0 and 24 h using a DeltaPix 200 Digital Camera. The width of the scratches was measured at each time point and quantified using Microsoft Excel computer program.

SPHERE FORMING ASSAY

OVCA 433 (10^4 cells) untreated, cisplatin, and cisplatin +U0126-treated cells were seeded on low attachment 24-well plates in normal growth medium. The sphere forming ability of the cells was photographed over 21 days using a phase contrast microscope (Axiovert 100, Zeiss, Germany) and assessed with the DeltaPix Viewer software (Denmark). Cellular aggregates with a diameter larger than 0.5 mm were classified as spheres.

RNA EXTRACTION AND REAL-TIME PCR

RNA extractions were performed using Trizol (Life Technologies, USA) using the Qiashredder and Rneasy kits (QIAGEN, Australia) according to manufacturer's instructions. The concentration and purity of RNA was determined using spectrophotometry (Nanodrop ND-1000 spectrophotometer, Thermo Scientific, USA) and 0.5 μg of RNA was used for cDNA synthesis. cDNA synthesis was performed using Superscript VILO (Invitrogen) according to manufacturer's instructions. Quantitative determination of mRNA levels of various genes was performed in triplicate using SYBR green (Applied Biosystems, Australia).

The following pairs of primers (forward/reverse) were used: E-cadherin (Entrez Gene ID 999, approved symbol CDH1) 5′-GCCCTGCCAATCCCGATGAAA/-3′-GGGGTCAGTATCAGCCGCT; vimentin (Entrez Gene ID 7431, approved symbol VIM) 5′-GCTTCAGAGAGAGGAAGCCGAAAA/-3′-CCGTGAGGTCAGGCTTGGAAA; Snail (Entrez Gene ID 6615, approved symbol SNAI1) 5′-CCAGACCCACTCAGATGTCAAGAA/-3′-GGCAGAGGACACAGAACCAGAAAA; Slug (Entrez Gene ID 6591, approved symbol SNAI2) 5′-CCCAATGGCCTCTCTCCTCTTT/-3′-CATCGCAGTGCAGCTGCTTATGTTT; Twist (Entrez Gene ID 7291, approved symbol TWIST1) 5′-CTAGAGACTCTGGAGCTGGATAACTAAAAA/-3′-CGACCTCTTGAGAATGCATGAAAAA; Oct-4 (Entrez Gene ID 5460, approved symbol POU5F1) 5′-CTTGCTGCAGAAGTGGGTGGAGGAA/-3′-CTGCAGTGTGGGTTTCGGGCA; Nanog (Entrez Gene ID 79923, approved symbol NANOG) 5′-CAGAAGGCCTCAGCACCTACCTA CCC CAGCC/-3′-TCTCTGCAGTCCTGCATGCAGTTCCAGCCAAA; MMP-2 (Entrez Gene ID 4313, approved symbol MMP2) 5′-CGGCCGCAGTGACGGAAA/-3′-CATCCTGGGACAGACGGAAG; MMP-9 (Entrez Gene ID 4318, approved symbol MMP9) 5′-TTGACAGCGACAAGAAGTGG/-3′-TATTCCTGCTGCATTACCG. qPCR and data collection was performed on an Applied Biosystems 7500 analyser. All quantifications were normalized to the mRNA expression of GAPDH (OVCA 433 cell line) (Entrez Gene ID 2597, approved symbol GAPDH) 5′-GGGGAGCCAAAAGGGTCATCATCT/-3′-GACGCCTGCTTCACCACCTTCTTG and 18S (PTs and ATs) (Entrez Gene ID 100008588, approved symbol RN18S1) 5′-GTAACCCGTTGAACCCCATT/3′-CCATCCAATCGGTAGTAGCG.

CELLS STAINING AND XENOTRANSPLANTATION INTO ZEBRAFISH EMBRYOS

This was performed as described previously [Marques et al., 2009]. Briefly, OVCA 433 cells, either untreated or treated with cisplatin or cisplatin +U0126, were stained with the fluorescent dye CM-Dil (Invitrogen) and injected as a single-cell suspension (~100 cells) into the yolk sac of 2 day old dechorionated and anesthetized zebrafish embryos. Embryos were examined 1 h post-injection (hpi) to confirm successful injections and incubated at 35°C for further analysis. Visualization of the cells inside zebrafish body was captured by a confocal microscope (Olympus FluoView 1000, Australia). Cell migration into the tail region was enumerated at 24 and 48 hpi. The study was approved by the Animal Research Ethics Committee (AEC # A73/2010) of Deakin University, Geelong, Melbourne, Australia.

STATISTICAL ANALYSIS

Student's *t*-test was used for the statistical analyses of migration (in vitro and in vivo) and qPCR analysis. Data are presented as mean ± SEM. A probability level of $P < 0.05$ was adopted throughout to determine statistical significance. Treatment groups were compared with the control group using one way-ANOVA and Dunnett's Multiple Comparison post-tests.

RESULTS

CISPLATIN-INDUCED MORPHOLOGICAL CHANGES WERE CONSISTENT WITH EMT

Treatment with different concentrations of cisplatin resulted in a loss of cell polarity in epithelioid untreated cells and was consistent with fibroblast-like spindle-shaped morphology in treated cells (Fig. 1). The change in cell morphology was cisplatin dose-dependent and varied with the cell type used. PTs were more vulnerable to cisplatin and the morphological changes were evident at cisplatin concentrations of 1–10 μg/ml within 3 days (GI50 ~ 1–2.5 μg/ml) (Fig. 1A). On the other hand, ATs were more resistant to cisplatin and morphological changes could be induced at concentrations between 5 and 10 μg/ml of cisplatin within 5 days [GI50 for chemonaive AT ~2.5 μg/ml, chemoresistant ATs ~7.5–10 μg/ml (Fig. 1B)]. In the OVCA 433 cell line cisplatin-induced morphological changes were evident at concentrations between 1 and 10 μg/ml (GI50 ~ 7 μg/ml) (Fig. 1C). Similar changes in the morphology were observed in the OVCA 433ST, OVCA 433LT cell lines, which were selected for cisplatin resistance (Supplementary Fig. 1).

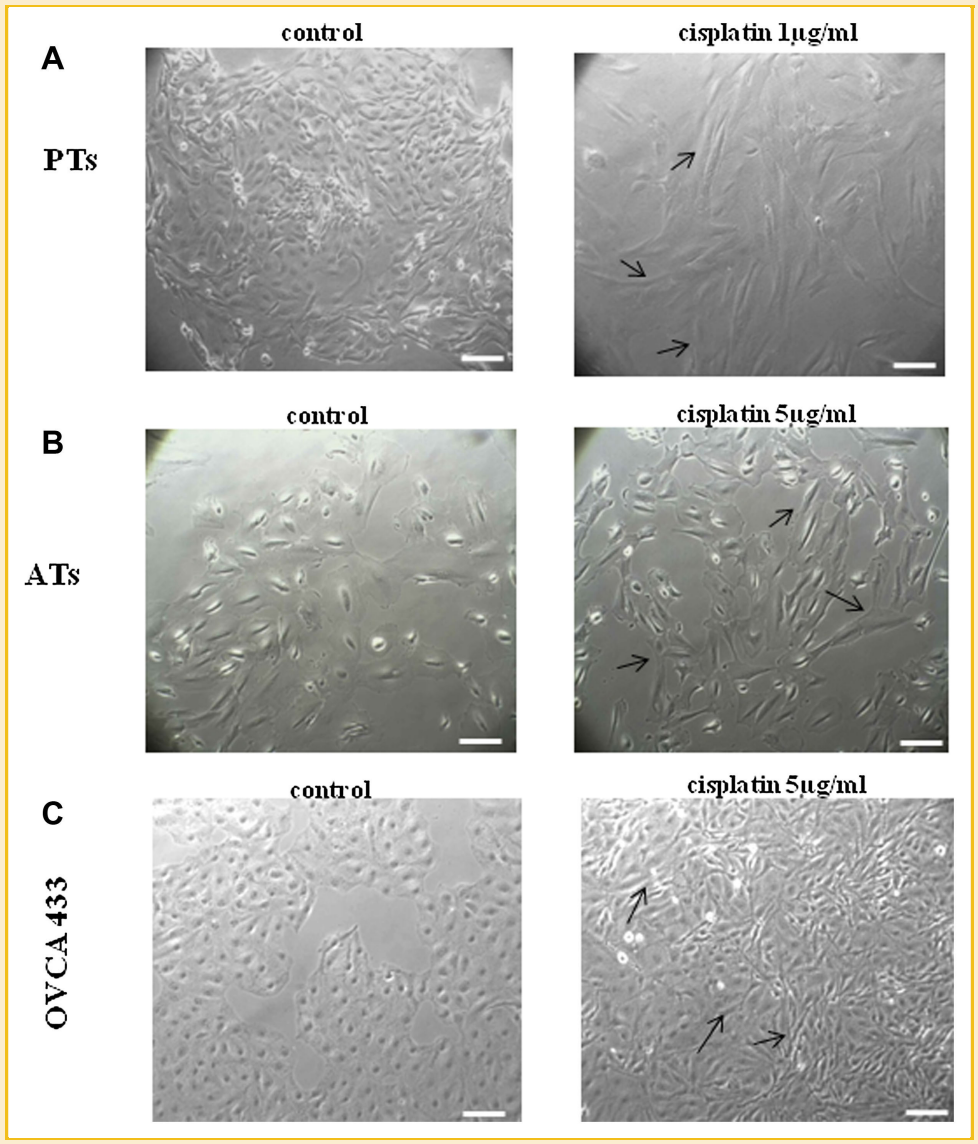

Fig. 1. A–C: Morphological features of PTs, ATs, and OVCA 433 cell line after treatment with cisplatin. The images were assessed by phase contrast microscope. Magnification—100×, scale bar = 50 μm. Arrows indicate cancer cells that have undergone EMT.

CISPLATIN-INDUCED MESENCHYMAL MORPHOLOGICAL CHANGES WERE ASSOCIATED WITH EMT MARKERS AT A PROTEIN LEVEL

To determine whether the changes in morphology in response to cisplatin involved molecular changes consistent with EMT, IF staining was performed on PTs and OVCA 433 cells while WB was performed on ATs and OVCA 433 cell lysates prepared in the presence and absence of cisplatin (Figs. 2 and 3). In these experiments PTs were treated with 1 μg/ml (3 days), ATs 5 μg/ml (5 days), and OVCA 433 cells 5 μg/ml of cisplatin (5 days). The expression of E-cadherin and N-cadherin in PTs and OVCA 433 cells was not confined to cell–cell junction but was rather diffuse and cytoplasmic. Similar expression of vimentin was observed in PTs but in OVCA 433 cells it was confined to peripheral membrane (Fig. 2). Cisplatin treatment led to a decrease in the expression of E-cadherin and increased N-cadherin and vimentin expression in ovarian cancer cells. These observations were confirmed further by WB in ATs (Fig. 3). Significantly increased expression of N-cadherin and vimentin was evident in cisplatin-treated ATs and OVCA 433 cell lysates compared to cell lysates prepared from untreated control cells (Fig. 3A,B). In parallel, the expression of E-cadherin was reduced in cisplatin-treated ATs compared to untreated ATs (Fig. 3A). E-cadherin cleavage has been reported previously in ovarian carcinomas [Symowicz et al., 2007]). ATs demonstrate both full length (120 kDa) and cleaved forms (80 kDa) of E-cadherin and the expression of both bands decreased with cisplatin treatment. As we have previously reported [Lim et al., 2007], the expression of E-cadherin in OVCA 433 cells was low and could not be determined by WB (Fig. 3B). Low expression of E-cadherin in

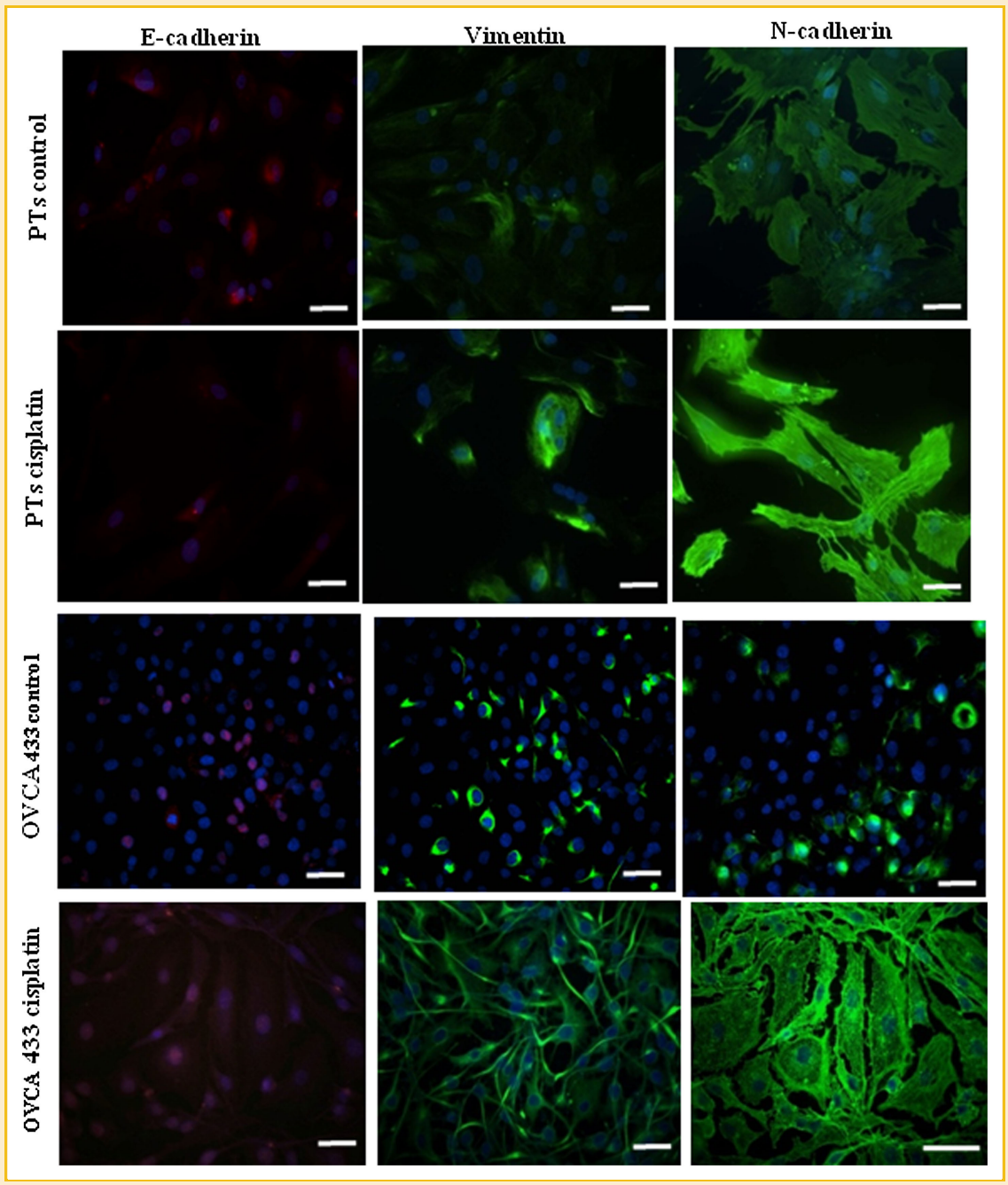

Fig. 2. Expression and immunolocalization of E-cadherin, N-cadherin, and vimentin in PTs and OVCA 433 cell line in response to cisplatin. The images were evaluated using rabbit polyclonal antibodies (red) or mouse monoclonal antibodies (green) as described in the "Materials and Methods" Section. Cellular and nuclear staining were visualized using secondary Alexa 488 (green) or 590 (red) fluorescent labeled antibody and DAPI (blue). Images are representative of three independent experiments. Magnification—200×; scale bar = 50 μm.

OVCA 433 cells may suggest that some degree of EMT may exist in these cells.

CISPLATIN-INDUCED MESENCHYMAL MORPHOLOGICAL CHANGES WERE ASSOCIATED WITH EMT MARKERS AT THE MRNA LEVEL

To determine if the changes in EMT-associated markers were consistent at the mRNA levels, qPCR was performed on cDNA prepared from RNA extracted from PTs and OVCA 433 cells treated with or without cisplatin. In these experiments, PTs were treated with 1 μg/ml of cisplatin (3 days) while OVCA 433 cells were treated with 5 or 10 μg/ml (5 days). OVCA 433ST and OVCA 433LT were also included in these experiments. Consistent with IF results, E-cadherin expression was significantly down regulated in PTs treated with cisplatin (Fig. 4A). Compared to control untreated cells, 10 μg/ml (5 days) cisplatin-treated OVCA 433 cells demonstrated significant decrease in E-cadherin mRNA levels (Fig. 4B). These observations

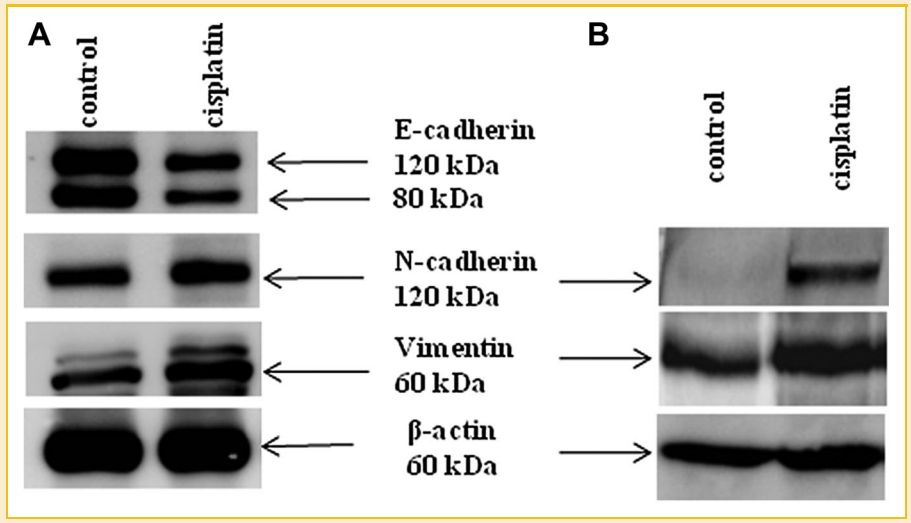

Fig. 3. Western blot analysis of E-cadherin, N-cadherin, and vimentin expression in (A) ATs and (B) OVCA 433 cells in response to cisplatin. Cell lysates were prepared and resolved by 10% SDS–PAGE gels as described in the "Materials and Methods" Section. Blots were probed with the primary and secondary antibodies, stripped and re-probed with mouse monoclonal β-actin antibody as an internal protein control. Images are representative of three independent samples.

were consistent in OVCA 433ST and OVCA 433LT cells compared to untreated control (Fig. 4B). Even though the mRNA expression of E-cadherin at 5 μg/ml cisplatin was decreased in OVCA 433 cells, it was not significant compared to control untreated cells. The mRNA expression of Slug, Snail, and Twist were significantly increased in response to cisplatin in PTs (Fig. 4A). A similar trend in Slug and Twist was observed in the OVCA 433 cell line (Fig. 4B) but the expression of Snail remained unchanged within the 5 days treatment. Snail expression however, was significantly enhanced in OVCA 433ST and OVCA 433LT cells (Fig. 4B). Consistent with that, the expression of vimentin was significantly enhanced in response to cisplatin in PTs and OVCA 433 cells (Fig. 4A,B).

CISPLATIN ENHANCED THE MIGRATORY POTENTIAL OF OVARIAN CANCER CELLS

Cisplatin also induced a motile phenotype in ovarian cancer cells as evaluated by the wound-healing assay in OVCA 433 cell line (Fig. 5). In the absence of cisplatin, 15% wound closure was observed in OVCA 433 cells after 24 h, compared to 35% wound closure in the presence of 5 μg/ml cisplatin under similar conditions (Fig. 5A). As the deregulation of cell motility contributes to invasive phenotype of cancer cells, we next investigated whether cisplatin-induced EMT in OVCA 433 cells is associated with the induction of expression of matrix metalloproteases (MMPs) known to disrupt the epithelial basement membranes in order to make way for migratory cells [Egeblad and Werb, 2002]. As expected there was a significant increase in the mRNA of MMP2 (Fig. 5B). There was an increased trend in the mRNA expression for MMP-9 in cisplatin-treated cells compared to control untreated cells but it was not significant (Fig. 5B). Gelatin zymography on tumor conditioned medium demonstrated enhanced expression of both pro-MMP-9 (92 kDa) and pro-MMP-2 (72 kDa) in cisplatin-treated samples (Fig. 5C). The expression of active MMP-9 (84 kDa) and active MMP-2 (64 kDa) were also observed in cisplatin-treated samples suggesting that treatment of ovarian cancer cells with cisplatin enhances the MMP2/9 mediated proteolytic pathways.

CISPLATIN ENHANCES THE CELL SURFACE EXPRESSION OF CSC MARKERS

As few recent studies have linked EMT with CSC-like phenotype [Mani et al., 2008], we assessed the cell surface expression of some known CSC markers by FC and IF in response to cisplatin treatment. In these experiments ATs were treated with 2.5 or 5 μg/ml of cisplatin (5 days) and OVCA 433 cells were treated with 5 μg/ml of cisplatin (5 days). Moderate expression of CD44, CD24, and α2 integrin subunit was evident by FC in ATs, while low expression of EpCAM was observed (Fig. 6A). Under these conditions, no expression of CD117 or CD133 was observed. However, in response to cisplatin (2.5 μg/ml, 5 days), an increase in the expression of CD44 and EpCAM was observed (Fig. 6A) but no increase in the expression of α2 integrin subunit, CD24, CD133, and CD117 was evident. On the other hand, enhanced expression of CD117 and CD133 was observed when ATs were treated with increased concentration of cisplatin (5 μg/ml) for the same time frame (Fig. 6A). No enhancement in the expression of α2 integrin subunit and CD24 was observed under these conditions.

The expression of CSC in response to cisplatin treatment was also confirmed by IF staining in PTs. In cisplatin-treated cells the expression of stemness proteins (CD117, CD133, and EpCAM) was not confined to the cell membrane but were scattered throughout the cells and only evident in certain populations of cells (Supplementary Fig. 2). The stemness characteristics of ATs as well as OVCA 433 cells were further assessed for the expression of pluripotent embryonic stem cell markers Oct-4 and Nanog by IF and qPCR (Fig. 6B,C). Enhanced expression of Oct-4 and Nanog in response to cisplatin (5 μg/ml, 5 days) was evident by the diffuse cytoplasmic and nuclear staining in majority of cisplatin-treated surviving ATs (Fig. 6B). These results were confirmed at the mRNA level in OVCA 433 cell

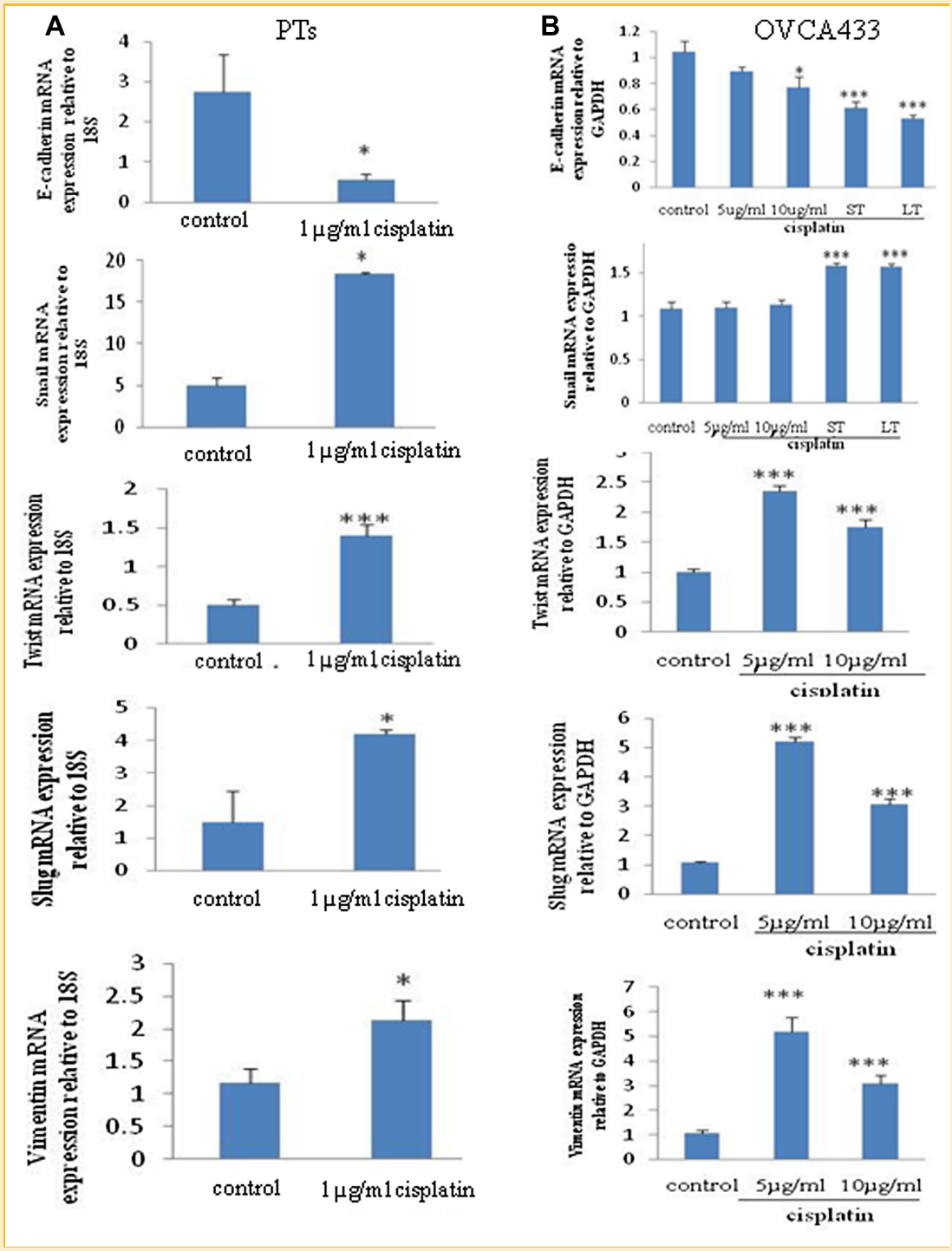

Fig. 4. mRNA expression of E-cadherin, Slug, Snail, and Twist in PTs and OVCA 433 cell line in response to cisplatin. A,B: PTs and OVCA 433 cells were treated with or without cisplatin, RNA was extracted, cDNA was prepared and qPCR was performed using the respective primers as described in the "Materials and Methods" Section. The experiment was performed on different PTs and five independent OVCA 433 samples in triplicate. Significantly different in cisplatin-treated cells compared to control untreated cells, $^{*}P < 0.05$ and $^{***}P < 0.001$. [Color figure can be seen in the online version of this article, available at http://wileyonlinelibrary.com/journal/jcb]

line which demonstrated significant increase in Oct-4 and Nanog expression in cells post cisplatin treatment (Fig. 6C).

As sphere formation has been described as important features for the survival of stem cells [Bapat et al., 2005], we evaluated the sphere forming abilities of control and cisplatin-treated OVCA 433 cells. In long term, cisplatin-treated cells (5 µg/ml, 5 days) demonstrated greater ability to form spheres on low attachment plates (Fig. 7). Within 6 days both control and cisplatin-treated cells demonstrated abilities to form cellular aggregates, but the aggregates in cisplatin-treated cells were relatively bigger than

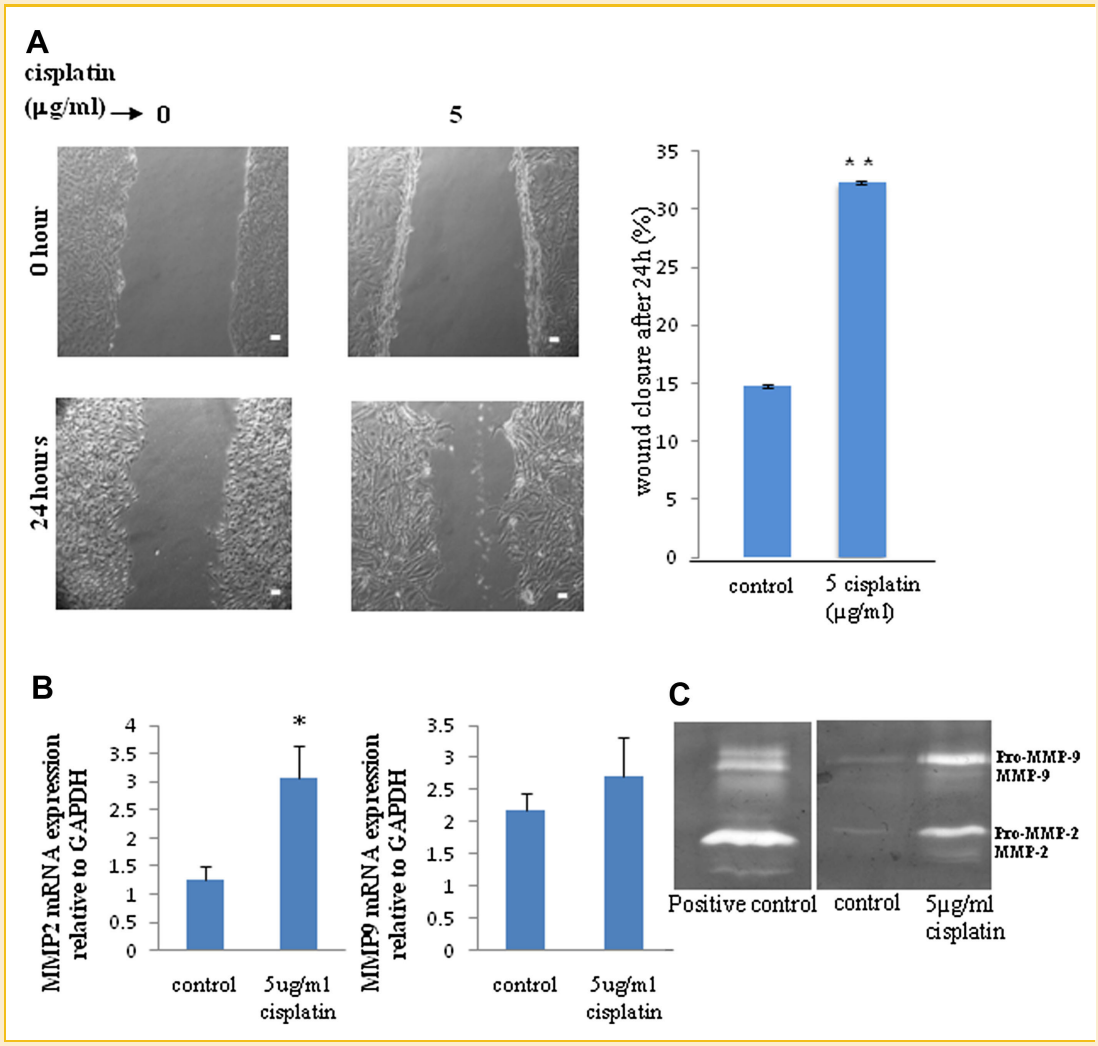

Fig. 5. Effect of cisplatin on the migration and MMP2/9 expression in OVCA 433 cells. A: The migratory abilities of OVCA 433 cells in the presence and absence of cisplatin was determined as described in the "Materials and Methods" Section. Phase contrast images are representative of one experiment repeated three times. The graphs represent percentage of wound closure from three independent experiments. Significantly different in cisplatin-treated cells compared to control untreated cells, $^{**}P < 0.01$. B: mRNA expression of MMP-2 and MMP-9 in the presence and absence of cisplatin was evaluated as described in Figure 4. mRNA expression of MMP-2 in OVCA 433 cells treated with cisplatin compared to control untreated cells, $^{*}P < 0.05$. C: Gelatin zymography demonstrating the amounts of pro-MMP-2, pro-MMP-9, active MMP-2 and MMP-9 secreted in the conditioned medium from untreated and cisplatin (5 μg/ml, 5 days) treated OVCA 433 cells. The results are representative of two independent experiments. [Color figure can be seen in the online version of this article, available at http://wileyonlinelibrary.com/journal/jcb]

control untreated cells (Fig. 7). Within 21 days, the aggregates formed by cisplatin-treated cells took the shape of compact spheres and were relatively bigger and twofold greater in numbers than control cells (control 21.3 ± 0.3, cisplatin treatment 42.3 ± 2.3). Most control cellular aggregates disintegrated within the 21 days time frame resulting in their decreased numbers compared to cisplatin-treated samples. These results suggest that cisplatin transformed residual cells are enriched in self-renewing cells as evidenced by their greater ability to survive in anchorage independent condition.

ACTIVATION OF THE ERK2 PATHWAY WAS ASSOCIATED WITH AN EMT AND CSC-LIKE PHENOTYPE

OVCA 433 cells displayed an increase in the activation of ERK1/2 and the expression of total (T)-ERK after 4 days of cisplatin treatment (5 μg/ml for 5 days) (Fig. 8A). The expression of P-ERK2 was significantly enhanced in response to cisplatin compared to control untreated cells (Fig. 8B). The expression of T-ERK2 also increased but was not significant (Fig. 8B). U0126 (10 μM), a highly selective MEK1 and MEK2 inhibitor, significantly inhibited cisplatin-induced ERK2 activation but had no effect on ERK1 activation (Fig. 8A,B). Under these conditions the expression of total T-ERK was also inhibited (Fig. 8A,B).

To further evaluate a direct role of ERK2 in cisplatin-induced chemoresistance we assessed the expression of selected EMT and CSC markers in the absence and presence of U0126. Inhibition of the ERK2 pathway by U0126 sensitized OVCA 433 cells to cisplatin-induced cell death and also inhibited cisplatin-induced migration (Fig. 8C). In the presence of cisplatin and U0126 significant abrogation of cisplatin induced increases in Slug, Twist

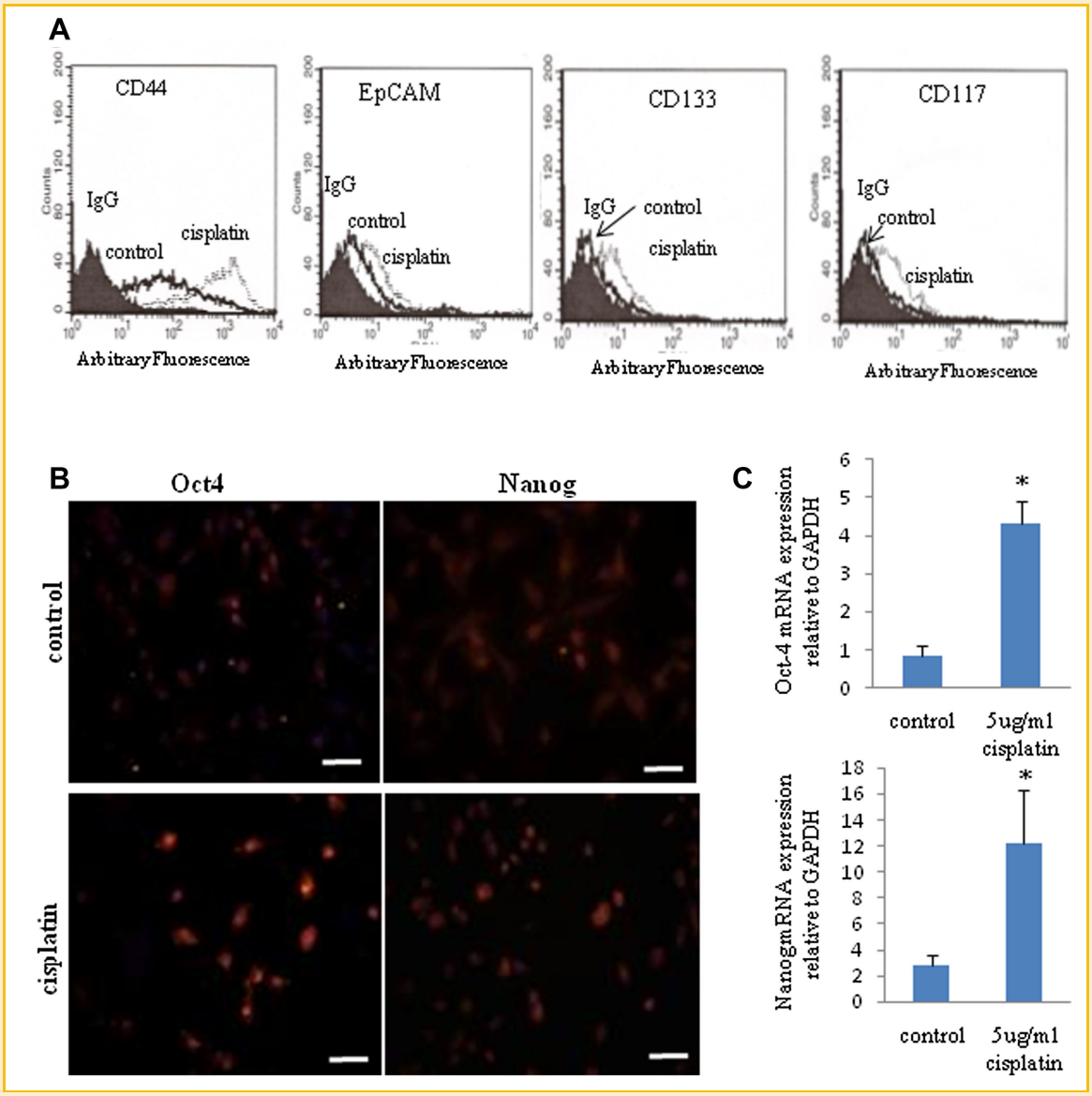

Fig. 6. Effect of cisplatin on the expression of CSC-like markers in ATs and OVCA 433 cells. A: The expression of CSC was assessed in ATs by FC. Untreated or cisplatin-treated cells were incubated with either control IgG or relevant primary antibodies against the respective CSC-like markers followed by secondary goat anti-mouse IgG conjugated with phycoerythrin. The filled histogram in each figure is control IgG, black lines indicate protein expression in control cells while broken lines demonstrate protein expression in cisplatin-treated cells. Results are representative of five independent samples. B: Expression and immunolocalization of Oct-4 and Nanog in ATs in response to cisplatin was performed as described in Figure 2. Magnification—200×; scale bar = 50 μm. C: Effect of cisplatin on the mRNA expression of Oct-4 and Nanog in OVCA 433 cell line was performed as described in Figure 4. Significantly different in cisplatin-treated cells compared to control untreated cells, $^{*}P < 0.05$.

(Supplementary Fig. 3), and vimentin expression was observed (Fig. 8D). U0126 also inhibited the induction of Oct-4 expression (Fig. 8D).

To confirm the in vivo relevance of the effects of U0126 on cisplatin-induced EMT phenotype, we employed an established zebrafish xeno-transplantation model of metastatic behavior [Marques et al., 2009]. Cells were fluorescently labeled prior to injection into the yolk sac of 2-day-old zebrafish embryos and visualized by confocal microscopy. Distinct fluorescent cells were observed from 12 hpi predominantly in the tail region (Fig. 8E, Supplementary Fig. 4), in a pattern similar to that observed with pancreatic tumor cells [Marques et al., 2009]. Cell migration into the tail was analyzed and quantified at both 24 and 48 hpi (Fig. 8E). In three independent experiments, the average numbers of cisplatin-induced EMT transformed cells migrating towards the tail of zebrafish were significantly more than the control untreated cells (Fig. 8E). U0126 inhibited the migration of cisplatin-treated cells to below the basal levels (Fig. 8E).

DISCUSSION

One of the greatest impediments in improving the survival rates of ovarian cancer patients after chemotherapy treatment has been a lack of understanding of the mechanisms by which residual tumor

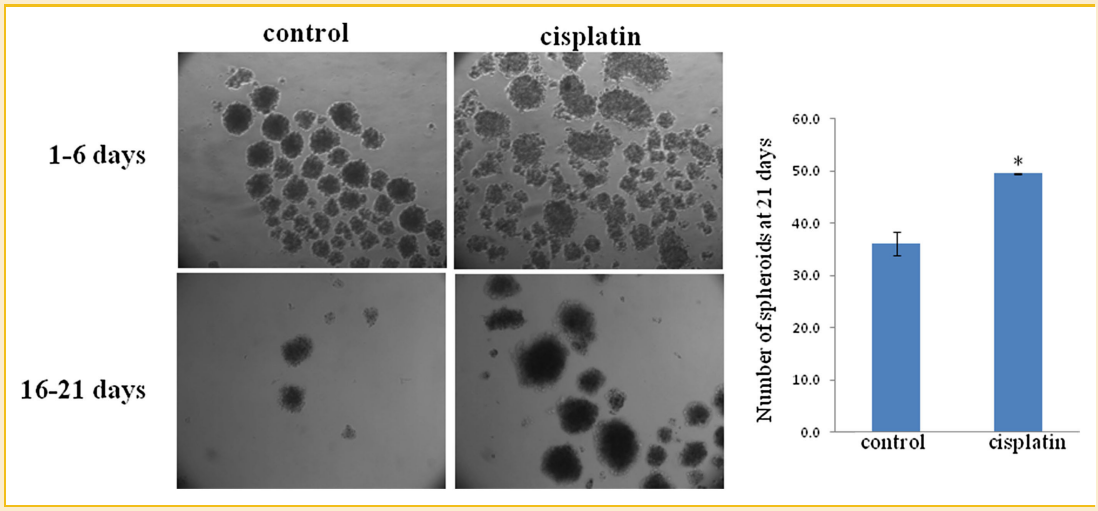

Fig. 7. Effect of cisplatin on the sphere forming ability of OVCA 433 cells. The sphere-forming assay was performed on low attachment plates as described in the "Materials and Methods" Section. The total numbers of spheres were counted in the 24-wells after 21 days as described in the Methods and Materials. Significantly different in cisplatin-treated cells compared to control untreated cells, $^{*}P < 0.05$. The experiment was performed three times in triplicate. Images are representative of a section of a 24-well.

cells survive after chemotherapy. Therefore, a systematic attempt is needed to model cisplatin and taxol responses, individually and in combination, on cells derived from human tumor samples to provide improved understanding of chemoresistance. The novelty of the present study is the use of primary and metastatic human ovarian tumor cells to dissect cellular mechanisms responsible for survival and the subsequent regrowth of cisplatin surviving residual tumor cells which ultimately are responsible for recurrence in ovarian cancer patients. As much recognized, there is a limitation on the availability of human tissues. Hence, to meet experimental needs we have expanded purified tumor cells and standardized the experimental protocol within 3–4 passages which take ~2 weeks. However, we have recently started isolating fresh tumor cells from larger volume of ascites (within 3 days) and we observe similar phenotypic changes in the context of EMT and CSC-like phenotypes in response to cisplatin, (data not shown) suggesting that that the effect of cisplatin can be consistently reproduced in vitro cultures.

We demonstrate that cisplatin treatment of PTs or metastatic epithelial ovarian tumor cells (ATs), and an ovarian cancer cell line, generated in each case a population of residual cells with combined features of EMT and CSC. Cisplatin-induced EMT not only caused transition from epitheloid to spindle-shaped fibroblast-like mesenchymal cells, but also resulted in changes in EMT marker profile reminiscent of "classical EMT" [Guarino et al., 2007]. Decreased expression of E-cadherin, and increased N-cadherin and vimentin, correlated with a significant increase in the expression of transcription factors such as Snail, Slug, and Twist that strongly repress the expression of E-cadherin. Lack of cell–cell junction expression of E- and N-cadherin in OVCA 433 cells was consistent with the diffuse cytoplasmic expression of these proteins in PTs. The fact that these cancer cells are not involved in maintaining specific tissue architecture and have de-regulated functions may explain these aberrant expressions. However, enhanced expression of E-cadherin repressing transcription factors in response to cisplatin treatment is a good indicator of the ongoing EMT process in these tumor cells. The fact that E-cadherin expression does not significantly decrease at low cisplatin concentration (5 μg/ml) but does at higher concentration (10 μg/ml), after multiple (OVCA 433ST), and long-term treatments (OVCA 433LT) may suggest that the EMT-mediated decrease in E-cadherin expression in OVCA 433 cells are dependent on DNA damage response elicited by higher concentrations or consecutive or long-term treatments by DNA damage agents. Similar scenario may be applicable for Snail expression but may not apply to the change in the expression of Slug and Twist which are more susceptible to cisplatin treatment. These transcription factors have been demonstrated to be frequently expressed in different cancers [Micalizzi et al., 2010], including ovarian cancer [Kurrey et al., 2005] and are expressed independent of each other in a cell type specific manner. Consistent with that, Snail, Slug, and Twist have been shown to confer resistance to chemotherapy and radiotherapy in cancer cells [Kurrey et al., 2009]. Induction of EMT in cisplatin surviving residual tumor cells is also consistent with their significantly higher migratory capacity compared to control cells. Overall, cisplatin-treated residual ovarian cancer cells possessed traits of "classical EMT" suggesting that EMT represents a potentially important mechanism of survival of cisplatin-treated cells in the setting of ovarian cancer recurrence.

We demonstrate that the concentrations of cisplatin needed to facilitate EMT in ovarian cancer cells obtained from different sources (PTs, ATs, and OVCA 433 cells) varied. Longer exposure and increased concentration of cisplatin were needed in ATs compared to PTs to achieve EMT. This may be due to the altered intrinsic mechanisms in ATs induced by the growth factor rich microenvironment of ascites impacting on the signaling networks and also the context in which tumor cells respond to therapy [Lane et al., 2007]. ATs from patients with recurrent ovarian tumors may have acquired

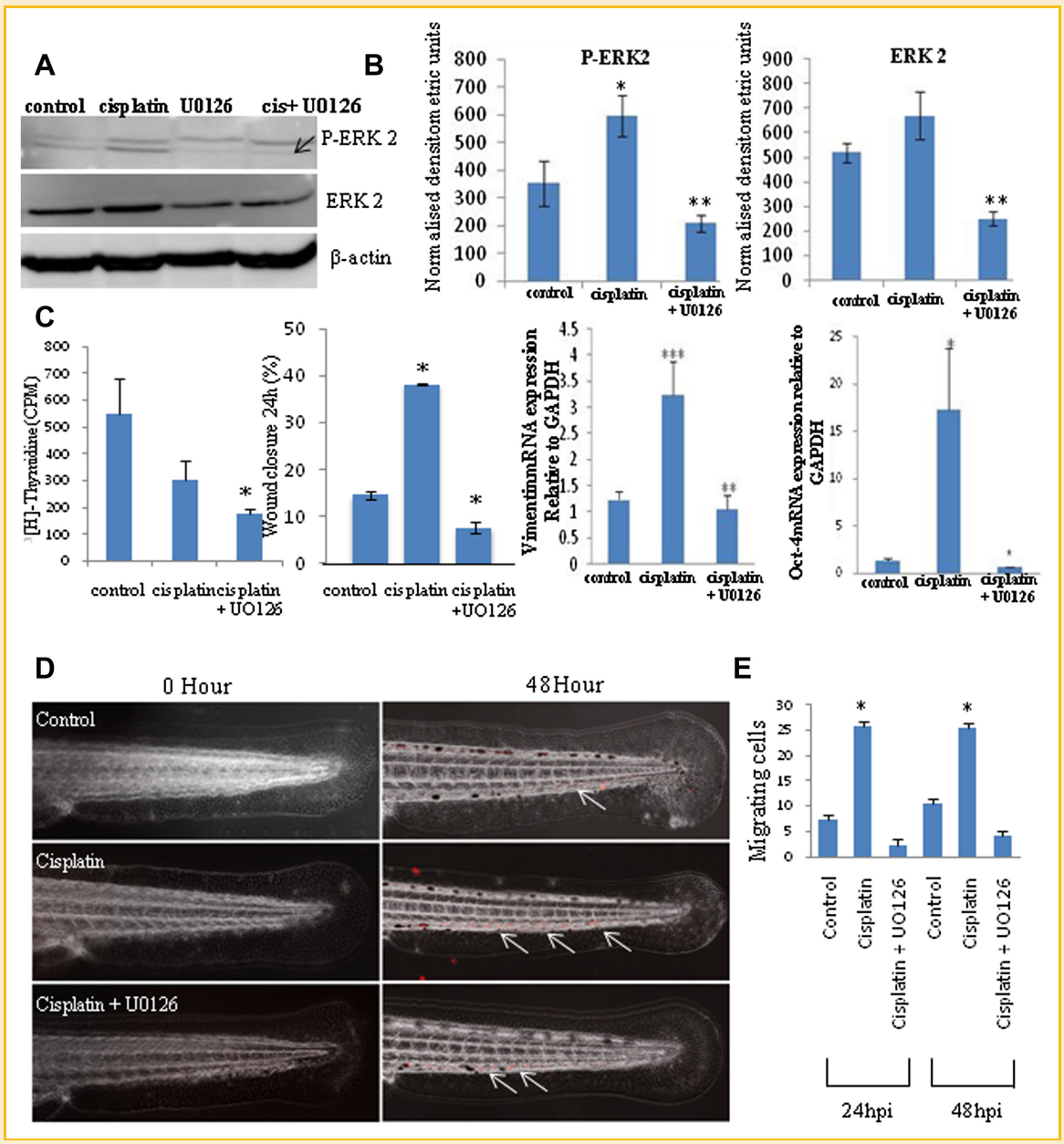

Fig. 8. Effect of U0126 on cisplatin-induced ERK2 mediated functions in OVCA 433 cells. A: Western blotting on control untreated, cisplatin treated, U0126 treated (10 μM), and cisplatin (5 μg/ml) and U0126 (10 μM)-treated cell lysates was performed as described in "Materials and Methods" Section. Results are representative of three independent experiments. B: Semi-quantitative densitometric analysis was performed to determine the expression of P-ERK2 and T-ERK2 normalized to β-actin using Image Quant software. Graphs are a representation of three independent experiments. Significantly different in cisplatin-treated cells compared to control cells, $^{*}P < 0.05$, and cisplatin-treated cells compared to cisplatin +U0126-treated cells, $^{**}P < 0.01$. C: Effect of U0126 on the proliferation ([^{3}H]-thymidine uptake) and in vitro wound closure assay of control and cisplatin-treated cells. Graphs are a representation of one experiment performed independently three times. Significantly different in cisplatin-treated cells compared to control untreated cells, $^{*}P < 0.05$. Significantly different in cisplatin +U0126-treated cells compared to cisplatin-treated cells, $^{*}P < 0.05$. D: Effect of U0126 on cisplatin-induced vimentin and Oct-4 mRNA expression in OVCA 433 cells. mRNA expression was evaluated as described in "Materials and Methods" Section. Significantly different in cisplatin-treated cells compared to control untreated cells, $^{***}P < 0.001$ and $^{*}P < 0.05$. Significantly different in cisplatin +U0126-treated cells compared to cisplatin-treated cells, $^{*}P < 0.05$ and $^{**}P < 0.001$. E: The migratory ability of control untreated and cisplatin-treated OVCA 433 cells were evaluated by xenotransplantaion in zebrafish embryos. Zebrafish embryos were injected with CM-DiI labeled OVCA433 cells that had been untreated, treated with cisplatin or treated with cisplatin +U0126, with the tail region imaged at 0 and 48 hpi. Migrating cells demonstrated in white arrows. F: Quantification of fluorescent cells in the tail region of zebrafish at 24 and 48 hpi. Significantly different in cisplatin-treated cells compared to control untreated cells, $^{*}P < 0.05$. [Color figure can be seen in the online version of this article, available at http://wileyonlinelibrary.com/journal/jcb]

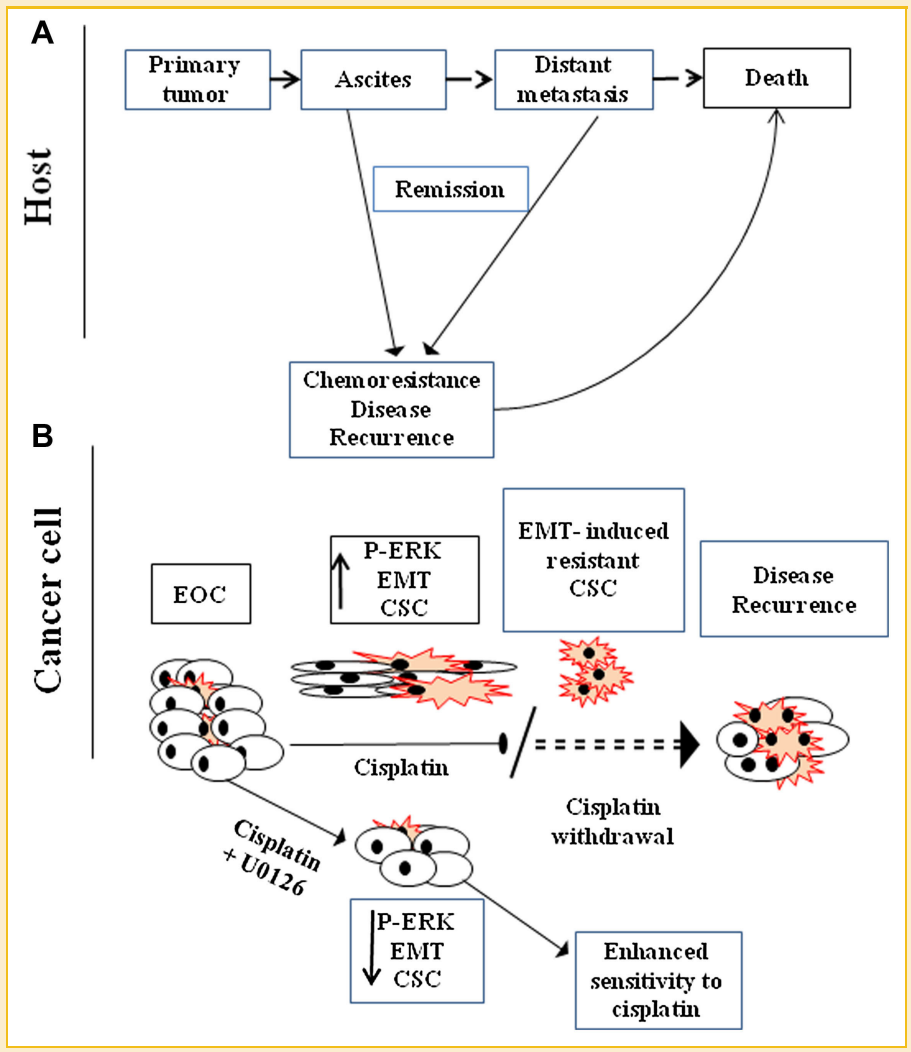

Fig. 9. Model of epithelial ovarian cancer cells surviving cisplatin-induced cytotoxicity. A: Primary tumor cells are shed into the ascites where they form distant metastasis leading to patient's death barring intervention. Cisplatin-based intervention (solid arrow) leads to short lived remission followed by recurrence leading to patient death. B: Cisplatin surviving residual cells undergo ERK2 pathway-associated EMT and CSC-like changes. U0126 blocks cisplatin-induced ERK2 activation and sensitizes residual cells to increased cell death. [Color figure can be seen in the online version of this article, available at http://wileyonlinelibrary.com/journal/jcb]

cisplatin resistance due to increased expression of nucleotide excision repair pathway proteins making them unsusceptible to low concentrations of cisplatin. Excision repair cross complementation 1 (ERCC1) has been associated with cisplatin resistance in ovarian tumors and cancer cell lines [Dabholkar et al., 1994; Selvakumaran et al., 2003]. Recent clinical trials suggest that patients with low ERCC1 levels benefit preferentially from cisplatin-based chemotherapy [Olaussen et al., 2006].

Enhanced expression of established CSC markers of breast cancer (CD44) [Al-Hajj et al., 2003], neuroblastomas (EpCAM) [Baeuerle and Gires, 2007], and prostate cancer ($\alpha 2$ integrin subunit) [Collins et al., 2001] after treatment with cisplatin suggest an association between EMT and CSC-like phenotype in cisplatin surviving residual ovarian cancer cells. As CD44 has been shown to interact with EpCAM [Baeuerle and Gires, 2007] and is required for the engagement of matrix derived survival signals through CD44-integrin axis [Lee et al., 2008], it is reasonable to expect that the expression of these molecules is dependent on each other and can be triggered by concentrations of cisplatin that initiate EMT-dependent cell–matrix interactions, cell motility, and the disruption of adherent junctions. Lack of enhancement of $\alpha 2$ integrin expression in ATs in response to cisplatin treatment may reflect an in vivo situation where cell–ECM interaction mediated signaling may not play an active role. On the other hand, generation of $CD133^{+}$ and $CD117^{+}$ cells in a more resistant cisplatin residual populations is consistent with their previous correlation with chemoresistance in ovarian carcinomas [Raspollini et al., 2004; Baba et al., 2009] and their involvement in distant metastasis [Adhikari et al., 2010] and tumor niche formation [Cui et al., 2010]. In addition, enhanced expression of Oct-4 and Nanog and sphere forming ability in response to cisplatin further reiterates the self-renewal and survival roles of these residual cells.

We also demonstrated that ERK2 signaling is associated in sensitizing OVCA 433 cells to cisplatin-induced cell death by suppressing cisplatin-induced EMT. In contrast, inhibition of ERK2 by U0126 had no effect on the expression of CD44 but inhibited cisplatin-enhanced expression of Oct-4 and sphere forming ability of residual cells. Using a robust in vivo xeno-transplantation model we have demonstrated enhanced migratory, invasive, and metastatic ability of cisplatin transformed cells. The observed enhanced migration of cisplatin-transformed cells in zebrafish reflects the intrinsic metastatic ability of these cells. The fact that a fraction of cisplatin-transformed cells (greater in number than the control) invade through the zebrafish body and translocate to the tail represents a valid indication of the capacity of these surviving cells to colonize to distant sites. These results are consistent with other animal models where only a small subset (~2%) of metastatic cells has been shown to survive and colonize at distant sites [Weiss, 1990]. The fact that U0126 was able to inhibit the translocation ability of cisplatin-transformed cells in vivo provides further evidence of the critical role of ERK in cisplatin-induced EMT. Hence, assessment of the migratory and invasive abilities of cisplatin-transformed cells in the zebrafish model can complement long-term mouse models and is valuable in evaluating the therapeutic efficacy of agents (such as U0126) against particular targets (such as ERK). Overall, our data suggest that targeting of ERK2 signaling may predispose cisplatin-surviving tumors to chemotherapy. Consistent with that, two recent articles have demonstrated the role of ERK-dependent pathways in enhancing antitumor efficacy of cisplatin chemotherapy [Basu et al., 2009; Sheridan et al., 2010].

In conclusion, our data for the first time provides a strong molecular link between cisplatin resistance, EMT and CSC in EOC. We hypothesize that in the course of chemotherapy treatment residual ovarian tumor cells acquire EMT and CSC-like phenotypes. Low cisplatin concentration initiates EMT and CSC by facilitating matrix remodeling to provide motility of residual cells to migrate to a distant site. However, subsequent increases in cisplatin concentration generate CSC with additional phenotypes (CD133, CD117), which provide growth advantage to the very few surviving residual cells in the form of niche formation to facilitate tumor recurrence. Hence, chemotherapy-treated cancer cells undergo a series of alterations with respect to "stemness" and it is the most resistant population of cells that are capable of regenerating the tumors leading to recurrence. On the basis of our results a model of cisplatin-induced chemoresistance in ovarian carcinomas is described in Figure 9.

ACKNOWLEDGMENTS

The authors wish to thank Royal Women's Hospital Foundation, Women's Cancer Foundation, National Health and Medical Research Council of Australia (JKF, RegKey#441101) and Victorian Breast Cancer Research Consortium (EWT) for supporting this work. AL and KA are the recipients of Royal Women's Hospital Scholarship and Australian Postgraduate Award. The authors also wish to acknowledge the help of Ms. Julene Hallo in the acquisition of clinical samples.

REFERENCES

Adhikari AS, Agarwal N, Wood BM, Porretta C, Ruiz B, Pochampally RR, Iwakuma T. 2010. CD117 and Stro-1 identify osteosarcoma tumor-initiating cells associated with metastasis and drug resistance. Cancer Res 70(11):4602–4612.

Ahmed N, Pansino F, Clyde R, Murthi P, Quinn MA, Rice GE, Agrez MV, Mok S, Baker MS. 2002. Overexpression of alpha(v)beta6 integrin in serous epithelial ovarian cancer regulates extracellular matrix degradation via the plasminogen activation cascade. Carcinogenesis 23(2):237–244.

Ahmed N, Riley C, Oliva K, Stutt E, Rice GE, Quinn MA. 2003. Integrin-linked kinase expression increases with ovarian tumour grade and is sustained by peritoneal tumour fluid. J Pathol 201/2:229–237.

Ahmed N, Thompson EW, Quinn MA. 2007. Epithelial-mesenchymal interconversions in normal ovarian surface epithelium and ovarian carcinomas: An exception to the norm. J Cell Physiol 213(3):581–588.

Ahmed N, Latifi A, Riley CB, Findlay JK, Quinn MA. 2010a. Neuronal transcription factor Brn-3a(l) is over expressed in high-grade ovarian carcinomas and tumor cells from ascites of patients with advanced-stage ovarian cancer. J Ovarian Res 3/1:17.

Ahmed N, Abubaker K, Findlay J, Quinn M. 2010b. Epithelial mesenchymal transition and cancer stem cell-like phenotypes facilitate chemoresistance in recurrent ovarian cancer. Curr Cancer Drug Targets 10(3):268–278.

Al-Hajj M, Wicha MS, Benito-Hernandez A, Morrison SJ, Clarke MF. 2003. Prospective identification of tumorigenic breast cancer cells. Proc Natl Acad Sci USA 100(7):3983–3988.

Baba T, Convery PA, Matsumura N, Whitaker RS, Kondoh E, Perry T, Huang Z, Bentley RC, Mori S, Fujii S, Marks JR, Berchuck A, Murphy SK. 2009. Epigenetic regulation of CD133 and tumorigenicity of CD133+ ovarian cancer cells. Oncogene 28(2):209–218.

Baeuerle PA, Gires O. 2007. EpCAM (CD326) finding its role in cancer. Br J Cancer 96(3):417–423.

Bapat SA, Mali AM, Koppikar CB, Kurrey NK. 2005. Stem and progenitor-like cells contribute to the aggressive behavior of human epithelial ovarian cancer. Cancer Res 65(8):3025–3029.

Basu S, Harfouche R, Soni S, Chimote G, Mashelkar RA, Sengupta S. 2009. Nanoparticle-mediated targeting of MAPK signaling predisposes tumor to chemotherapy. Proc Natl Acad Sci USA 106(19):7957–7961.

Brozovic A, Osmak M. 2007. Activation of mitogen-activated protein kinases by cisplatin and their role in cisplatin-resistance. Cancer Lett 251(1):1–16.

Collins AT, Habib FK, Maitland NJ, Neal DE. 2001. Identification and isolation of human prostate epithelial stem cells based on alpha(2)beta(1)-integrin expression. J Cell Sci 114(Pt 21):3865–3872.

Colomiere M, Ward AC, Riley C, Trenerry MK, Cameron-Smith D, Findlay J, Ackland L, Ahmed N. 2009. Cross talk of signals between EGFR and IL-6R through JAK2/STAT3 mediate epithelial–mesenchymal transition in ovarian carcinomas. Br J Cancer 100(1):134–144.

Cui W, Yazlovitskaya EM, Mayo MS, Pelling JC, Persons DL. 2000. Cisplatin-induced response of c-jun N-terminal kinase 1 and extracellular signal-regulated protein kinases 1 and 2 in a series of cisplatin-resistant ovarian carcinoma cell lines. Mol Carcinog 29(4):219–228.

Cui L, Ohuchida K, Mizumoto K, Moriyama T, Onimaru M, Nakata K, Nabae T, Ueki T, Sato N, Tominaga Y, Tanaka M. 2010. Prospectively isolated cancer-associated CD10 fibroblasts have stronger interactions with CD133 colon cancer cells than with CD133 cancer cells. PLoS One 5(8): e12121.

Dabholkar M, Vionnet J, Bostick-Bruton F, Yu JJ, Reed E. 1994. Messenger RNA levels of XPAC and ERCC1 in ovarian cancer tissue correlate with response to platinum-based chemotherapy. J Clin Invest 94(2):703–708.

Egeblad M, Werb Z. 2002. New functions for the matrix metalloproteinases in cancer progression. Nat Rev Cancer 2/3:161–164.

Guarino M, Rubino B, Ballabio G. 2007. The role of epithelial–mesenchymal transition in cancer pathology. Pathology 39(3):305–318.

Hayakawa J, Ohmichi M, Kurachi H, Kanda Y, Hisamoto K, Nishio Y, Adachi K, Tasaka K, Kanzaki T, Murata Y. 2000. Inhibition of BAD phosphorylation either at serine 112 via extracellular signal-regulated protein kinase cascade or at serine 136 via Akt cascade sensitizes human ovarian cancer cells to cisplatin. Cancer Res 60(21):5988–5994.

Jayachandran G, Ueda K, Wang B, Roth JA, Ji L. 2010. NPRL2 sensitizes human non-small cell lung cancer (NSCLC) cells to cisplatin treatment by regulating key components in the DNA repair pathway. PLoS One 5(8): e11994.

Kajita M, McClinic KN, Wade PA. 2004. Aberrant expression of the transcription factors snail and slug alters the response to genotoxic stress. Mol Cell Biol 24(17):7559–7566.

Kim MR, Choi HK, Cho KB, Kim HS, Kang KW. 2009. Involvement of Pin1 induction in epithelial–mesenchymal transition of tamoxifen-resistant breast cancer cells. Cancer Sci 100(10):1834–1841.

Kunimura C, Kikuchi K, Ahmed N, Shimizu A, Yasumoto S. 1998. Telomerase activity in a specific cell subset co-expressing integrinbeta1/EGFR but not p75NGFR/bcl2/integrin beta4 in normal human epithelial cells. Oncogene 17(2):187–197.

Kurrey NK, K A, Bapat SA. 2005. Snail and Slug are major determinants of ovarian cancer invasiveness at the transcription level. Gynecol Oncol 97(1):155–165.

Kurrey NK, Jalgaonkar SP, Joglekar AV, Ghanate AD, Chaskar PD, Doiphode RY, Bapat SA. 2009. Snail and Slug mediate radio- and chemo-resistance by antagonizing p53-mediated apoptosis and acquiring a stem-like phenotype in ovarian cancer cells. Stem Cells 27(9):2059–2068.

Lala PK, Lee BP, Xu G, Chakraborty C. 2002. Human placental trophoblast as an in vitro model for tumor progression. Can J Physiol Pharmacol 80(2):142–149.

Lane D, Robert V, Grondin R, Rancourt C, Piche A. 2007. Malignant ascites protect against TRAIL-induced apoptosis by activating the PI3K/Akt pathway in human ovarian carcinoma cells. Int J Cancer 121(6):1227–1237.

Lee S, Yoon S, Kim DH. 2007. A high nuclear basal level of ERK2 phosphorylation contributes to the resistance of cisplatin-resistant human ovarian cancer cells. Gynecol Oncol 104(2):338–344.

Lee JL, Wang MJ, Sudhir PR, Chen JY. 2008. CD44 engagement promotes matrix-derived survival through the CD44-SRC-integrin axis in lipid rafts. Mol Cell Biol 28(18):5710–5723.

Leong CO, Vidnovic N, DeYoung MP, Sgroi D, Ellisen LW. 2007. The p63/p73 network mediates chemosensitivity to cisplatin in a biologically defined subset of primary breast cancers. J Clin Invest 117(5):1370–1380.

Lim R, Ahmed N, Borregaard N, Riley C, Wafai R, Thompson EW, Quinn MA, Rice GE. 2007. Neutrophil gelatinase-associated lipocalin (NGAL) an early-screening biomarker for ovarian cancer: NGAL is associated with epidermal growth factor-induced epithelio-mesenchymal transition. Int J Cancer 120(11):2426–2434.

Lombaerts M, van Wezel T, Philippo K, Dierssen JW, Zimmerman RM, Oosting J, van Eijk R, Eilers PH, van de Water B, Cornelisse CJ, Cleton-Jansen AM. 2006. E-cadherin transcriptional downregulation by promoter methylation but not mutation is related to epithelial-to-mesenchymal transition in breast cancer cell lines. Br J Cancer 94(5):661–671.

Mabuchi S, Ohmichi M, Nishio Y, Hayasaka T, Kimura A, Ohta T, Saito M, Kawagoe J, Takahashi K, Yada-Hashimoto N, Sakata M, Motoyama T, Kurachi H, Tasaka K, Murata Y. 2004. Inhibition of NFkappaB increases the efficacy of cisplatin in in vitro and in vivo ovarian cancer models. J Biol Chem 279(22):23477–23485.

Mani SA, Guo W, Liao MJ, Eaton EN, Ayyanan A, Zhou AY, Brooks M, Reinhard F, Zhang CC, Shipitsin M, Campbell LL, Polyak K, Brisken C, Yang J, Weinberg RA. 2008. The epithelial–mesenchymal transition generates cells with properties of stem cells. Cell 133(4):704–715.

Marques IJ, Weiss FU, Vlecken DH, Nitsche C, Bakkers J, Lagendijk AK, Partecke LI, Heidecke CD, Lerch MM, Bagowski CP. 2009. Metastatic behaviour of primary human tumours in a zebrafish xenotransplantation model. BMC Cancer 9:128.

Micalizzi DS, Farabaugh SM, Ford HL. 2010. Epithelial–mesenchymal transition in cancer: Parallels between normal development and tumor progression. J Mammary Gland Biol Neoplasia 15(2):117–134.

Ning Y, Zeineldin R, Liu Y, Rosenberg M, Stack MS, Hudson LG. 2005. Down-regulation of integrin alpha2 surface expression by mutant epidermal growth factor receptor (EGFRvIII) induces aberrant cell spreading and focal adhesion formation. Cancer Res 65/20:9280–9286.

Ohmichi M, Hayakawa J, Tasaka K, Kurachi H, Murata Y. 2005. Mechanisms of platinum drug resistance. Trends Pharmacol Sci 26(3):113–116.

Olaussen KA, Dunant A, Fouret P, Brambilla E, Andre F, Haddad V, Taranchon E, Filipits M, Pirker R, Popper HH, Stahel R, Sabatier L, Pignon JP, Tursz T, Le Chevalier T, Soria JC. 2006. DNA repair by ERCC1 in non-small-cell lung cancer and cisplatin-based adjuvant chemotherapy. N Engl J Med 355(10):983–991.

Ozols RF. 2006. Systemic therapy for ovarian cancer: Current status and new treatments. Semin Oncol 33(2 Suppl 6):S3–11.

Peinado H, Olmeda D, Cano A. 2007. Snail, Zeb and bHLH factors in tumour progression: An alliance against the epithelial phenotype? Nat Rev Cancer 7(6):415–428.

Perego P, Giarola M, Righetti SC, Supino R, Caserini C, Delia D, Pierotti MA, Miyashita T, Reed JC, Zunino F. 1996. Association between cisplatin resistance and mutation of p53 gene and reduced bax expression in ovarian carcinoma cell systems. Cancer Res 56(3):556–562.

Raspollini MR, Amunni G, Villanucci A, Baroni G, Taddei A, Taddei GL. 2004. c-KIT expression and correlation with chemotherapy resistance in ovarian carcinoma: An immunocytochemical study. Ann Oncol 15(4):594–597.

Sedletska Y, Giraud-Panis MJ, Malinge JM. 2005. Cisplatin is a DNA-damaging antitumour compound triggering multifactorial biochemical responses in cancer cells: Importance of apoptotic pathways. Curr Med Chem Anticancer Agents 5(3):251–265.

Selvakumaran M, Pisarcik DA, Bao R, Yeung AT, Hamilton TC. 2003. Enhanced cisplatin cytotoxicity by disturbing the nucleotide excision repair pathway in ovarian cancer cell lines. Cancer Res 63(6):1311–1316.

Sheridan C, Brumatti G, Elgendy M, Brunet M, Martin SJ. 2010. An ERK-dependent pathway to Noxa expression regulates apoptosis by platinum-based chemotherapeutic drugs. Oncogene 29(49):6428–6441.

Silverberg SG. 2000. Histopathologic grading of ovarian carcinoma: A review and proposal. Int J Gynecol Pathol 19(1):7–15.

Symowicz J, Adley BP, Gleason KJ, Johnson JJ, Ghosh S, Fishman DA, Hudson LG, Stack MS. 2007. Engagement of collagen-binding integrins promotes matrix metalloproteinase-9-dependent E-cadherin ectodomain shedding in ovarian carcinoma cells. Cancer Res 67(5):2030–2039.

Uchikado Y, Natsugoe S, Okumura H, Setoyama T, Matsumoto M, Ishigami S, Aikou T. 2005. Slug Expression in the E-cadherin preserved tumors is related to prognosis in patients with esophageal squamous cell carcinoma. Clin Cancer Res 11(3):1174–1180.

Wang Z, Li Y, Kong D, Banerjee S, Ahmad A, Azmi AS, Ali S, Abbruzzese JL, Gallick GE, Sarkar FH. 2009. Acquisition of epithelial–mesenchymal transition phenotype of gemcitabine-resistant pancreatic cancer cells is linked with activation of the notch signaling pathway. Cancer Res 69(6):2400–2407.

Weiss L. 1990. Metastatic inefficiency. Adv Cancer Res 54:159–211.